Adaptive Trajectory Tracking During Motorized and FES-Induced Biceps Curls via Integral Concurrent Learning

Brendon C. Allen*, Kimberly J. Stubbs*, Warren E. Dixon*

***Abstract*—A common rehabilitative technique for those with neuromuscular disorders is functional electrical stimulation (FES) induced exercise such as FES-induced biceps curls. Closed-loop control of a motorized FES system presents numerous challenges since the system has nonlinear and uncertain dynamics and switching is required between motor and FES control, which is further complicated by the muscle having an uncertain control effectiveness. In this paper, data-based, opportunistic learning is achieved by implementing an integral concurrent learning (ICL) controller during a motorized and FES-induced biceps curl exercise. A Lyapunov-based analysis is performed to ensure exponential trajectory tracking and opportunistic, exponential learning of the uncertain human and machine parameters. In addition to improved tracking performance and robustness the potential of learning the specific dynamics of a person during a rehabilitative exercise could be clinically significant. Preliminary simulation results are provided and demonstrate an average position error of 0.14 $\pm$ 1.17 deg and an average velocity error of 0.004 $\pm$ 1.18 deg/s.**

***Index Terms*—Functional electrical stimulation (FES), integral concurrent learning (ICL), parameter identification, switched systems, rehabilitation robotics, Lyapunov methods.**

I. Introduction

Functional electrical stimulation (FES) induced exercise is commonly used for rehabilitation of those with neuromuscular disorders [1]. One application of FES is FES-induced biceps curls [2]–[5]. However, there are numerous challenges associated with closed-loop control of FES-induced biceps curls. For example, the dynamics are uncertain and nonlinear [6], high levels of stimulation (i.e., pulse width) can be uncomfortable, and the muscle control effectiveness is uncertain [7]. For rehabilitative systems including hybrid exoskeletons [8], further complications result from the need to control switching between a motor and FES of a muscle.

Closed-loop FES controllers have been developed for various rehabilitative methods, such as leg extensions [9]–[12], rowing [13], walking [8], cycling [14]–[18], and upper-body movement [2]–[5] among others. A common technique used for closed-loop FES controllers is to use high-gain and or high (infinite) frequency feedback to ensure robustness despite uncertainties in the system (cf. [2], [4], [5], [9], [10]). Such robust control methods are further motivated because they typically yield a negative definite derivative of a strict Lyapunov function, which facilitates the development of switched systems analysis methods, including the development of dwell-time conditions. However, such robust control methods result in an accelerated onset of fatigue due to high frequency of stimulation and can be uncomfortable [15]. Motivated by the goal of reducing the high-gain and high-frequency feedback components of FES controllers, various results have developed adaptive feedforward terms to augment FES controllers (cf. [8], [11], [13]–[18]). Results such as [12], [13], and [18] approximate the uncertain dynamics using fuzzy logic or neural networks (NN) up to some residual error by using model-free feedforward terms. The results in [14]–[17] take advantage of the fact that cycling is a repetitive and periodic task by using repetitive learning control (RLC) or iterative learning control (ILC) to exploit past control inputs to improve the tracking performance. In contrast to such model-free control methods, results such as [8] and [11] exploit knowledge of the dynamics to develop model-based adaptive controllers.

For some applications, it is preferred for the adaptive controller to not only improve tracking performance, but to also learn or identify the parameters of the system. In general, such an objective requires satisfying the persistence of excitation (PE) condition; traditional adaptive controllers yield asymptotic tracking results with no guarantee of parameter identification [19]. In [20], it is shown that adaptive controllers without PE can exhibit a bursting phenomenon, which results in periods of unstable or oscillatory behavior. Additionally, in general, it is not possible to verify the PE condition for nonlinear systems [19]. In recent years, methods were developed to perform model approximation online such as initial excitation (IE) [21] and concurrent learning (CL) [22]. IE uses a switched parameter estimator and low pass filters to relax the PE condition and yield exponential parameter convergence. CL has a finite excitation (FE) condition that is more mild than PE and can be satisfied online. CL works by using previous input and output data of the system to update the estimate of the unknown parameters, facilitating the potential for exponential stability. More recently, integral concurrent learning (ICL) [19], [23], and [24] was developed motivated by the fact that traditional CL requires the highest order derivative to be known [19] (which can be calculated

*Department of Mechanical and Aerospace Engineering, University of Florida, Gainesville FL 32611-6250, USA Email: {brendoncallen, kimberlyjstubbs, wdixon}@ufl.edu

This research is supported in part by the National Defense Science and Engineering Graduate Fellowship Program, the Assistant Secretary of Defense for Health Affairs, through the Congressionally Directed Medical Research Program under Award No. W81XWH1910330, and NSF award number 1762829. Any opinions, findings and conclusions, or recommendations expressed in this material are those of the author(s) and do not necessarily reflect the views of the sponsoring agency.

numerically with a filter applied to reduce the noise).

To date no IE, CL, or ICL based controller has been developed for an FES system. Performing ICL on a motorized FES system has numerous benefits. For example, person specific dynamics can be identified in real time, which could have clinical significance and such methods can yield exponential results, which facilitate switched systems analysis that is inherent to many FES objectives. Additionally, adaptive control reduces high-gain/high-frequency feedback components, resulting in a more efficient FES controller with lower overall FES inputs, leading to a more comfortable experience and delaying the onset of fatigue [15].

In this paper, an ICL controller is developed for motorized and FES-induced biceps curls, and a Lyapunov-based analysis is performed to ensure exponential stability of the trajectory tracking and parameter estimate errors, eliminating the potential for bursting errors [19]. During the biceps curl, control is switched between FES and the motor during elbow flexion and extension, respectively. This switched control is further complicated by the fact that the control effectiveness of the muscle is unknown. The existence of switching between multiple control inputs, when at least one has an uncertain control effectiveness, creates a unique problem that differentiates the result in this paper from those of previous ICL results, such as those in [19], [23], and [24]. The solution is to utilize opportunistic learning where the parameters of each subsystem are learned while the subsystem is active. A preliminary simulation is performed to validate the performance of the designed control system and yields an average position error of 0.14 $\pm$ 1.17 deg and an average velocity error of 0.004 $\pm$ 1.18 deg/s. Efforts to perform preliminary experiments were stymied due to Covid-19. $\tilde{\theta}$ \tilde{\theta}

II. Dynamics

The nonlinear and uncertain arm-joint dynamics are modeled as in [5] as[1]

$$M\left(\ddot{q}\right)+G\left(q\right)+P\left(q,\dot{q}\right)+B_{d}\left(\dot{q}\right)=\tau_{m}\left(t\right)+\tau_{e}\left(t\right), \quad (1)$$

where $q : \mathbb{R}_{\geq 0} \to \mathcal{Q}$, $\dot{q} : \mathbb{R}_{\geq 0} \to \mathbb{R}$, and $\ddot{q} : \mathbb{R}_{\geq 0} \to \mathbb{R}$ denote the measurable forearm angle about the elbow joint, measurable angular velocity, and unmeasured acceleration, respectively, and the set of all possible forearm angles is denoted by $\mathcal{Q} \subseteq \mathbb{R}$. The inertial and gravitational effects, denoted by $M : \mathbb{R} \to \mathbb{R}_{>0}$ and $G : \mathcal{Q} \to \mathbb{R}$, respectively, are defined as

$$M\left(\ddot{q}\right)\triangleq J\ddot{q}, \quad G\left(q\right)\triangleq mgl\cos\left(q-\theta_{0}\right), \quad (2)$$

where $J, m, g, l \in \mathbb{R}_{>0}$ are unknown constants and $\theta_0 \in \mathbb{R}_{>0}$ is a known constant. The passive viscoelastic tissue effect and the hybrid exoskeleton bicep machine's viscous damping effect, denoted by $P : \mathcal{Q} \times \mathbb{R} \to \mathbb{R}$ and $B_d : \mathbb{R} \to \mathbb{R}$, respectively, are defined as

$$P\left(q,\dot{q}\right)\triangleq k_{e1}\left(q-k_{e2}\right)+b_{v}\dot{q}, \quad B_{d}\left(\dot{q}\right)\triangleq b_{d}\dot{q}, \quad (3)$$

where $k_{e1}, k_{e2}, b_v, b_d \in \mathbb{R}$, are unknown constants. The forearm-joint torque produced by FES and the motor are denoted by $\tau_m : \mathbb{R}_{\geq 0} \to \mathbb{R}$ and $\tau_e : \mathbb{R}_{\geq 0} \to \mathbb{R}$, respectively, and are defined as

$$\tau_{m}\left(t\right)\triangleq b_{m}u_{m}\left(t\right), \quad \tau_{e}\left(t\right)\triangleq b_{e}u_{e}\left(t\right), \quad (4)$$

where $b_m \in \mathbb{R}_{>0}$ is an unknown constant that denotes the muscle control effectiveness of the biceps brachii muscle group for a given electrode placement[2], and $b_e \in \mathbb{R}_{>0}$ denotes the known and constant motor control effectiveness. The FES input (i.e., pulse width), $u_m : \mathbb{R}_{\geq 0} \to \mathbb{R}$, and the motor input (i.e., current), $u_e : \mathbb{R}_{\geq 0} \to \mathbb{R}$, are respectively defined as

$$u_{m}\left(t\right)\triangleq k_{m}\sigma_{m}\left(t\right)u_{FES}\left(t\right), \quad u_{e}\left(t\right)\triangleq k_{e}\sigma_{e}\left(t\right)u_{mot}\left(t\right), \quad (5)$$

where $k_m, k_e \in \mathbb{R}_{>0}$ are selectable constants, and $u_{FES} : \mathbb{R}_{\geq 0} \to \mathbb{R}$ and $u_{mot} : \mathbb{R}_{\geq 0} \to \mathbb{R}$ denote the subsequently designed control inputs for the FES and motor, respectively. The FES and motor switching signals, denoted by $\sigma_m : \mathbb{R}_{\geq 0} \to \{0, 1\}$ and $\sigma_e : \mathbb{R}_{\geq 0} \to \{0, 1\}$, respectively, are defined as

$$\sigma_{m}\left(t\right)\triangleq\begin{cases}1, & \dot{q}_{d}\geq 0\\ 0, & \text{otherwise}\end{cases}, \quad (6)$$

$$\sigma_{e}\left(t\right)\triangleq\begin{cases}1, & \dot{q}_{d}<0\\ 0, & \text{otherwise}\end{cases}, \quad (7)$$

where, $q_d : \mathbb{R}_{\geq 0} \to \mathbb{R}$, denotes the desired and sufficiently smooth (the first and second derivatives exist and are bounded) position trajectory, and $\dot{q}_d : \mathbb{R}_{\geq 0} \to \mathbb{R}$, denotes the desired velocity trajectory. The switching signals are designed such that FES is applied during elbow flexion and the motor is activated during elbow extension. Therefore, whenever $\sigma_m = 1$, $\sigma_e = 0$ and whenever $\sigma_e = 1$, $\sigma_m = 0$. Substituting (2), (4), and (5) into (1) yields[3]

$$B_{m}\sigma_{m}u_{FES}+B_{e}u_{mot}= \ J\ddot{q}+G+P+B_{d}, \quad (8)$$

where $B_m \triangleq b_m k_m$ and $B_e \triangleq b_e k_e \sigma_e$. The switched system in (8) has the following properties [1]. **Property 1:** $c_j \leq M \leq c_J$, where c_j, $c_J \in \mathbb{R}_{>0}$ are known constants. **Property 2:** The muscle control effectiveness b_m is lower and upper bounded and thus, $c_b \leq B_m \leq c_B$, where $c_b, c_B \in \mathbb{R}_{>0}$ are known constants. **Property 3:** The dynamics in (8) are linear in the unknown constant parameters and can be expressed as

$$Y_{1}\theta_{e}\triangleq J\ddot{q}+G+P+B_{d}, \quad (9)$$

[1]For notational brevity, all explicit dependence on time, t, within the terms $q(t)$, $\dot{q}(t)$, and $\ddot{q}(t)$ is suppressed.

[2]Due to the effects of changing muscle geometry, the muscle control effectiveness changes with the elbow angle. However, with proper electrode placement, stimulation of the bicep during curls can be segmented into distinct regions for each electrode, where over an electrode's respective region the muscle effectiveness can be approximated as a constant [3], [5]. In this paper, a single electrode is considered. Subsequent research will include multiple electrodes and switching between them with opportunistic learning of the muscle effectiveness at each electrode site.

[3]For notational brevity, all functional dependencies are hereafter suppressed unless required for clarity of exposition.

when only the motor is active (i.e., $\sigma_e = 1$ and $\sigma_m = 0$) and can be expressed as

$$Y_1\theta_m \triangleq \frac{1}{B_m}\left(J\ddot{q} + G + P + B_d\right), \tag{10}$$

when only FES is active (i.e., $\sigma_m = 1$ and $\sigma_e = 0$) , where $Y_1 \in \mathbb{R}^{1\times p}$, $B_m \in \mathbb{R}$, and $\theta_e, \theta_m \in \mathbb{R}^p$ denote the unknown constant parameters when in the motor and FES regions, respectively, and p is the number of uncertain parameters.

III. Control Development

A. Tracking Error Development

The control objective is for the forearm to track a desired trajectory and is quantified by a measurable position tracking error, denoted by $e_1 : \mathbb{R}_{\geq 0} \to \mathbb{R}$, and defined as

$$e_1 \triangleq q_d - q. \tag{11}$$

A measurable auxiliary tracking error, denoted by $e_2 : \mathbb{R}_{\geq 0} \to \mathbb{R}$, is designed as

$$e_2 \triangleq \dot{e}_1 + \alpha e_1, \tag{12}$$

where $\alpha \in \mathbb{R}_{>0}$ is a selectable constant. The open-loop error system is obtained by taking the derivative of (12), multiplying by J, and using (8) to yield

$$J\dot{e}_2 = \begin{cases} Y_2\theta_e - B_e u_{mot}, & \sigma_e = 1 \\ B_m\left(Y_2\theta_m - u_{FES}\right), & \sigma_m = 1 \end{cases}, \tag{13}$$

where θ_e and θ_m are the uncertain parameters defined in (9) and (10), respectively, and the measurable matrix $Y_2 \in \mathbb{R}^{1\times p}$ combined with θ_e is defined as

$$Y_2\theta_e \triangleq J\ddot{q}_d + G + P + B_d + \alpha J\dot{e}_1. \tag{14}$$

B. Parameter Identification Development

The motor and FES parameter identification errors, denoted by $\tilde{\theta}_e \in \mathbb{R}^p$ and $\tilde{\theta}_m \in \mathbb{R}^p$, respectively, are defined as

$$\tilde{\theta}_e \triangleq \theta - \hat{\theta}_e, \tag{15}$$

$$\tilde{\theta}_m \triangleq \theta - \hat{\theta}_m, \tag{16}$$

where the motor and FES parameter estimates are denoted by $\hat{\theta}_e \in \mathbb{R}^p$ and $\hat{\theta}_m \in \mathbb{R}^p$, respectively. The update laws for the motor and FES parameter estimates are designed based on the subsequent stability analysis as

$$\dot{\hat{\theta}}_e \triangleq \begin{cases} \Gamma_e Y_2^T e_2 + k_3\Gamma_e S_e, & \sigma_e = 1 \\ 0, & \sigma_{el} = 0 \\ k_3\Gamma_e S_e, & \sigma_{el} = 1 \end{cases}, \tag{17}$$

$$\dot{\hat{\theta}}_m \triangleq \begin{cases} \Gamma_m Y_2^T e_2 + k_4\Gamma_m S_m, & \sigma_m = 1 \\ 0, & \sigma_{ml} = 0 \\ k_4\Gamma_m S_m, & \sigma_{ml} = 1 \end{cases}, \tag{18}$$

where S_e and S_m are auxiliary terms defined as

$$S_e \triangleq \sum_{i=1}^{N_e} \mathcal{Y}_{ei}^T\left(\mathcal{U}_{ei} - \mathcal{Y}_{ei}\hat{\theta}_e\right), \tag{19}$$

$$S_m \triangleq \sum_{i=1}^{N_m} \mathcal{Y}_{mi}^T\left(\mathcal{U}_{mi} - \mathcal{Y}_{mi}\hat{\theta}_m\right), \tag{20}$$

where $k_3, k_4 \in \mathbb{R}_{>0}$ are selectable constants, $\Gamma_e, \Gamma_m \in \mathbb{R}^{p\times p}$ are selectable constant, positive definite and diagonal matrices, $N_e, N_m \in \mathbb{N}$ are constant integers denoting the size of the concurrent learning history stacks, and the switching signals, $\sigma_{el} : \mathbb{R}_{\geq 0} \to \{0,\, 1\}$ and $\sigma_{ml} : \mathbb{R}_{\geq 0} \to \{0,\, 1\}$, are respectively defined as

$$\sigma_{el}(t) \triangleq \begin{cases} 1 & \sigma_e = 0 \text{ and } \lambda_{min}\left\{\sum_{i=1}^{N_e} \mathcal{Y}_{ei}^T\mathcal{Y}_{ei}\right\} \geq \lambda_e \\ 0 & \sigma_e = 0 \text{ and } \lambda_{min}\left\{\sum_{i=1}^{N_e} \mathcal{Y}_{ei}^T\mathcal{Y}_{ei}\right\} < \lambda_e \end{cases}, \tag{21}$$

$$\sigma_{ml}(t) \triangleq \begin{cases} 1 & \sigma_m = 0 \text{ and } \lambda_{min}\left\{\sum_{i=1}^{N_m} \mathcal{Y}_{mi}^T\mathcal{Y}_{mi}\right\} \geq \lambda_m \\ 0 & \sigma_m = 0 \text{ and } \lambda_{min}\left\{\sum_{i=1}^{N_m} \mathcal{Y}_{mi}^T\mathcal{Y}_{mi}\right\} < \lambda_m \end{cases}, \tag{22}$$

where $\lambda_{min}\{\cdot\}$ ($\lambda_{max}\{\cdot\}$) denotes the minimum (maximum) eigenvalue of $\{\cdot\}$ and $\lambda_e, \lambda_m \in \mathbb{R}_{>0}$ are selectable constants. The motor ICL terms $\mathcal{Y}_{ei} \triangleq \mathcal{Y}_e(t_{ei})$ and $\mathcal{U}_{ei} \triangleq \mathcal{U}_e(t_{ei})$ are defined as

$$\mathcal{Y}_e(t) = \begin{cases} 0_{n\times 1} & \sigma_e = 0 \\ 0_{n\times 1} & t - t_n^e \in [0, \triangle t] \\ \int_{t-\triangle t}^{t} Y_1(\sigma)\, d\sigma & t - t_n^e > \triangle t \end{cases}, \tag{23}$$

$$\mathcal{U}_e(t) = \begin{cases} 0 & \sigma_e = 0 \\ 0 & t - t_n^e \in [0, \triangle t] \\ \int_{t-\triangle t}^{t} B_e u_{mot}(\sigma)\, d\sigma & t - t_n^e > \triangle t \end{cases}, \tag{24}$$

where $t_{ei} \in \left(t_n^e + \Delta t, t_{n+1}^m\right)$, $\forall n \in \{0, 1, 2, ...\}$, $0_{n\times 1}$ denotes a $n \times 1$ matrix of zeros, and $\triangle t \in \mathbb{R}_{>0}$ denotes a selectable constant that represents the size of the window of integration. The switching times are denoted by $\left\{t_n^i\right\}$, $i \in \{m,\, e\}$, $n \in \{0, 1, 2, ...\}$, which represent the instants in time when σ_m becomes nonzero $(i = m)$ and the instants when σ_e becomes nonzero $(i = e)$. The FES ICL terms $\mathcal{Y}_{mi} \triangleq \mathcal{Y}_m(t_{mi})$ and $\mathcal{U}_{mi} \triangleq \mathcal{U}_m(t_{mi})$ are defined as

$$\mathcal{Y}_m(t) = \begin{cases} 0_{n\times 1} & \sigma_m = 0 \\ 0_{n\times 1} & t - t_n^m \in [0, \triangle t] \\ \int_{t-\triangle t}^{t} Y_1(\sigma)\, d\sigma & t - t_n^m > \triangle t \end{cases}, \tag{25}$$

$$\mathcal{U}_m(t) = \begin{cases} 0 & \sigma_m = 0 \\ 0 & t - t_n^m \in [0, \triangle t] \\ \int_{t-\triangle t}^{t} \sigma_m u_{FES}(\sigma)\, d\sigma & t - t_n^m > \triangle t \end{cases}, \tag{26}$$

where $t_{mi} \in (t_n^m + \Delta t, t_n^e)$, $\forall n \in \{0, 1, 2, ...\}$. The auxiliary terms S_e and S_m contain a history stack of prior input and output data generated from the dynamics. When $t \in \left(t_n^e + \Delta t, t_{n+1}^m\right), \forall n$, substituting the definition of (9) into (8) and integrating both sides yields

$$\mathcal{Y}_{ei}\theta_e = \mathcal{U}_{ei}, \quad \forall t_{ei}. \tag{27}$$

Likewise, when $t \in (t_n^m + \Delta t, t_n^e), \forall n$, substituting the definition of (10) into (8) and integrating both sides yields

$$\mathcal{Y}_{mi}\theta_m = \mathcal{U}_{mi}, \quad \forall t_{mi}. \tag{28}$$

The ICL terms in (23)-(26) are designed to remove the dependence on acceleration. Integrating both sides of (9) yields

$$\int_{t-\triangle t}^{t} Y_1(\sigma)\theta_e d\sigma \triangleq Y_3\theta_e + \int_{t-\triangle t}^{t} Y_4(\sigma)\theta_e d\sigma, \tag{29}$$

$\forall t \in \left(t_n^e + \Delta t, t_{n+1}^m\right)$, $\forall n$, where the regression matrices $Y_3, Y_4 \in \mathbb{R}^{1\times p}$ are defined as

$$Y_3\theta_e \triangleq J\left(\dot{q}(t) - \dot{q}(t-\triangle t)\right), \tag{30}$$

$$Y_4\theta_e \triangleq G + P + B_d. \tag{31}$$

Likewise, integrating both sides of (10) yields

$$\int_{t-\triangle t}^{t} Y_1(\sigma)\theta_m d\sigma \triangleq Y_3\theta_m + \int_{t-\triangle t}^{t} Y_4(\sigma)\theta_m d\sigma, \tag{32}$$

$\forall t \in (t_n^m + \Delta t, t_n^e)$, $\forall n$, where

$$Y_3\theta_m \triangleq \frac{J}{B_m}\left(\dot{q}(t) - \dot{q}(t-\triangle t)\right), \tag{33}$$

$$Y_4\theta_m \triangleq \frac{1}{B_m}\left(G + P + B_d\right). \tag{34}$$

Motivated by [19], [23], and [24] the design of (30), (31), (33), and (34) allow for (23) and (25) to be calculated without requiring the acceleration to be measured. To facilitate the subsequent analysis, substituting (27) into (19) and using (15) and substituting (28) into (20) and using (16) yields the subsequent equivalent and non-implementable auxiliary equations

$$S_e = \sum_{i=1}^{N_e} \mathcal{Y}_{ei}^T \mathcal{Y}_{ei}\tilde{\theta}_e, \tag{35}$$

$$S_m = \sum_{i=1}^{N_m} \mathcal{Y}_{mi}^T \mathcal{Y}_{mi}\tilde{\theta}_m. \tag{36}$$

C. Closed-Loop Error System

Adaptive motor and FES controllers are designed based on (13) and the subsequent stability analysis respectively as

$$u_{mot} = \frac{1}{B_e}\left(Y_2\hat{\theta}_e + k_1 e_2 + e_1\right), \tag{37}$$

$$u_{FES} = Y_2\hat{\theta}_m + k_2 e_2, \tag{38}$$

where k_1, $k_2 \in \mathbb{R}_{>0}$ are selectable constants. Substituting (37) and (38) into (13) yields the closed-loop error system

$$J\dot{e}_2 = \begin{cases} Y_2\tilde{\theta}_e - k_1 e_2 - e_1, & \sigma_e = 1 \\ B_m\left(Y_2\tilde{\theta}_m - k_2 e_2\right), & \sigma_m = 1 \end{cases}. \tag{39}$$

IV. Stability Analysis

The design of the parameter estimate update laws in (17) and (18) allow for the traditional PE criteria for parameter identification to be relaxed to the FE criteria that is provided in Assumption 1.

Assumption 1. The system is sufficiently excited over a finite duration of time such that $\exists T_e, T_m \in \mathbb{R}_{>0}$ such that $\forall t \geq T_e, \lambda_{min}\left\{\sum_{i=1}^{N_e} \mathcal{Y}_{ei}^T\mathcal{Y}_{ei}\right\} \geq \lambda_e$ and $\forall t \geq T_m, \lambda_{min}\left\{\sum_{i=1}^{N_m} \mathcal{Y}_{mi}^T\mathcal{Y}_{mi}\right\} \geq \lambda_m$. Let $T \in \mathbb{R}_{>0}$ be defined as $T \triangleq \max(T_e, T_m)$.

A positive definite, continuously differentiable, common Lyapunov function candidate denoted by $V : \mathbb{R}^{2+2p} \to \mathbb{R}_{>0}$ is defined as

$$V \triangleq \frac{1}{2}e_1^2 + \frac{1}{2}Je_2^2 + \frac{1}{2}\tilde{\theta}_e^T\Gamma_e^{-1}\tilde{\theta}_e + \frac{1}{2}B_m\tilde{\theta}_m^T\Gamma_m^{-1}\tilde{\theta}_m, \tag{40}$$

which satisfies the following inequalities:

$$\lambda_1\|z\|^2 \leq V \leq \lambda_2\|z\|^2, \tag{41}$$

where $z \in \mathbb{R}^{2+2p}$ is defined as

$$z \triangleq \begin{bmatrix} e_1 & e_2 & \tilde{\theta}_e^T & \tilde{\theta}_m^T \end{bmatrix}^T, \tag{42}$$

and $\lambda_1, \lambda_2 \in \mathbb{R}_{>0}$ are known constants defined as

$$\lambda_1 \triangleq \frac{1}{2}\min\left(1, c_j, \lambda_{min}\left\{\Gamma_e^{-1}\right\}, c_b\lambda_{min}\left\{\Gamma_m^{-1}\right\}\right),$$

$$\lambda_2 \triangleq \frac{1}{2}\max\left(1, c_J, \lambda_{max}\left\{\Gamma_e^{-1}\right\}, c_B\lambda_{max}\left\{\Gamma_m^{-1}\right\}\right).$$

Theorem 1. *For the closed-loop error system defined in (39), the adaptive update laws and controllers defined in (17), (18), (37), and (38) yield bounded trajectory tracking errors and parameter estimation errors over the time interval $t \in [0, T)$, provided the following gain conditions are satisfied*

$$\alpha > \frac{1}{2}, \quad k_2 > \frac{1}{2c_b}. \tag{43}$$

Proof: The solution to the time derivative of (40) exists almost everywhere (a.e.) within $t \in [t_0, \infty)$, because the closed-loop error system in (39) and the update laws in (17) and (18) are discontinuous. A generalized time derivative of V, called $\dot{\tilde{V}}$, exists such that $\dot{V}(z) \overset{\text{a.e.}}{\in} \dot{\tilde{V}}(z)$. Let $z(t)$ for $t \in [t_0, \infty)$ be a Filippov solution to the differential inclusion $\dot{z} \in K[h](z)$ and let $h : \mathbb{R}^4 \to \mathbb{R}^4$ be defined as $h \triangleq \begin{bmatrix} \dot{e}_1 & \dot{e}_2 & \dot{\hat{\theta}}_e & \dot{\hat{\theta}}_m \end{bmatrix}^T$ [25]. Taking the time derivative of (40) and using (12) yields

$$\begin{aligned} \dot{\tilde{V}} \subseteq\ & e_1(e_2 - \alpha e_1) + e_2 K[J\dot{e}_2] - \tilde{\theta}_e^T\Gamma_e^{-1}K\left[\dot{\hat{\theta}}_e\right] \\ & - B_m\tilde{\theta}_m^T\Gamma_m^{-1}K\left[\dot{\hat{\theta}}_m\right], \end{aligned} \tag{44}$$

where $K[\cdot]$ is defined as in [26].

From the switching laws in (6) and (7) there are two cases: either only the motor is active ($\sigma_e = 1$ and $\sigma_m = 0$) or only FES is active ($\sigma_m = 1$ and $\sigma_e = 0$).

For the case when $\sigma_e = 1$, substituting (17), (18), (35), (36) and (39) into (44), canceling common terms, and using the fact that $\dot{V}(z) \overset{\text{a.e.}}{\in} \dot{\tilde{V}}(z)$, yields

$$\dot{V} \overset{\text{a.e.}}{=} \begin{cases} -\alpha e_1^2 - k_1 e_2^2 - k_3 \tilde{\theta}_e^T \sum_{i=1}^{N_e} \mathcal{Y}_{ei}^T \mathcal{Y}_{ei} \tilde{\theta}_e, & \sigma_{ml} = 0 \\ -\alpha e_1^2 - k_1 e_2^2 - k_3 \tilde{\theta}_e^T \sum_{i=1}^{N_e} \mathcal{Y}_{ei}^T \mathcal{Y}_{ei} \tilde{\theta}_e & \\ -k_4 B_m \tilde{\theta}_m^T \sum_{i=1}^{N_m} \mathcal{Y}_{mi}^T \mathcal{Y}_{mi} \tilde{\theta}_m, & \sigma_{ml} = 1 \end{cases}. \tag{45}$$

By Assumption 1, learning is not complete for $t \in [0, T)$, therefore $\sum_{i=1}^{N_e} \mathcal{Y}_{ei}^T \mathcal{Y}_{ei}$ and $\sum_{i=1}^{N_m} \mathcal{Y}_{mi}^T \mathcal{Y}_{mi}$ are positive semi-definite for at least a portion of $t \in [0, T)$. Therefore, (45) can be bounded above by

$$\dot{V} \overset{\text{a.e.}}{\leq} -\alpha e_1^2 - k_1 e_2^2, \tag{46}$$

$\forall t \in \left[t_n^e, t_{n+1}^m\right) \cap [0, T), \forall n$. For the case when $\sigma_m = 1$, substituting (17), (18), (35), (36) and (39) into (44) and canceling common terms yields

$$\dot{V} \overset{\text{a.e.}}{=} \begin{cases} -\alpha e_1^2 + e_1 e_2 - B_m k_2 e_2^2 & \\ -k_4 B_m \tilde{\theta}_m^T \sum_{i=1}^{N_m} \mathcal{Y}_{mi}^T \mathcal{Y}_{mi} \tilde{\theta}_m, & \sigma_{el} = 0 \\ -\alpha e_1^2 - B_m k_2 e_2^2 - k_3 \tilde{\theta}_e^T \sum_{i=1}^{N_e} \mathcal{Y}_{ei}^T \mathcal{Y}_{ei} \tilde{\theta}_e & \\ -k_4 B_m \tilde{\theta}_m^T \sum_{i=1}^{N_m} \mathcal{Y}_{mi}^T \mathcal{Y}_{mi} \tilde{\theta}_m + e_1 e_2, & \sigma_{el} = 1 \end{cases}. \tag{47}$$

Likewise, since learning is not complete for $t \in [0, T)$, (47) can be upper bounded by utilizing Property 2 and Young's Inequality as

$$\dot{V} \overset{\text{a.e.}}{\leq} -\left(\alpha - \frac{1}{2}\right) e_1^2 - \left(c_b k_2 - \frac{1}{2}\right) e_2^2, \tag{48}$$

$\forall t \in [t_n^m, t_n^e) \cap [0, T), \forall n$. An overall upper bound for both (46) and (48) can be obtained as

$$\dot{V} \overset{\text{a.e.}}{\leq} -\left(\alpha - \frac{1}{2}\right) e_1^2 - \beta e_2^2, \tag{49}$$

$\forall t \in [0, T)$, where $\beta \triangleq \min\left(k_1, c_b k_2 - \frac{1}{2}\right)$. Since $V \geq 0$ and $\dot{V} \leq 0$ it can be seen that $V \in \mathcal{L}_\infty$ and thus $e_1, e_2, \tilde{\theta}_e, \tilde{\theta}_m \in \mathcal{L}_\infty$. By the definitions in (15) and (16) and since $\tilde{\theta}_e, \tilde{\theta}_m \in \mathcal{L}_\infty$, then $\hat{\theta}_e, \hat{\theta}_m \in \mathcal{L}_\infty$, it can likewise be shown that $\dot{e}_1, q, \dot{q} \in \mathcal{L}_\infty$ and $Y_2 \in \mathcal{L}_\infty$, and thus, $u_{mot}, u_{FES} \in \mathcal{L}_\infty$. In fact, it can be shown by using (41) that

$$\|z(T)\| \leq \sqrt{\frac{\lambda_2}{\lambda_1}} \|z(0)\|. \tag{50}$$

■

Theorem 2. *For the closed-loop error system defined in (39), the adaptive update laws and controllers defined in (17), (18), (37), (38) yield exponential trajectory tracking errors and parameter estimation errors over the time interval $t \in [0, \infty)$ in the sense that*

$$\|z(t)\| \leq \frac{\lambda_2}{\lambda_1} \exp\left(\frac{\delta}{2\lambda_2} T\right) \|z(0)\| \exp\left(-\frac{\delta}{2\lambda_2} t\right), \tag{51}$$

provided the gain conditions in (43) are met, where T is defined in Assumption 1 and

$$\delta \triangleq \min\left(\alpha - \frac{1}{2}, k_1, c_b k_2 - \frac{1}{2}, k_3 \lambda_e, k_4 \lambda_m c_b\right).$$

Proof: By Assumption 1, $\lambda_{min}\left\{\sum_{i=1}^{N_e} \mathcal{Y}_{ei}^T \mathcal{Y}_{ei}\right\} \geq \lambda_e$ and $\lambda_{min}\left\{\sum_{i=1}^{N_m} \mathcal{Y}_{mi}^T \mathcal{Y}_{mi}\right\} \geq \lambda_m$ for all $t \in [T, \infty)$, which implies that $\sum_{i=1}^{N_e} \mathcal{Y}_{ei}^T \mathcal{Y}_{ei}$ and $\sum_{i=1}^{N_m} \mathcal{Y}_{mi}^T \mathcal{Y}_{mi}$ are both positive definite for all $t \in [T, \infty)$. Therefore, for the case when $\sigma_e = 1$, (45) can be upper bounded using Assumption 1 and Property 2 to yield

$$\dot{V} \overset{\text{a.e.}}{\leq} -\alpha e_1^2 - k_1 e_2^2 - k_3 \lambda_e \tilde{\theta}_e^T \tilde{\theta}_e - k_4 \lambda_m c_b \tilde{\theta}_m^T \tilde{\theta}_m, \tag{52}$$

$\forall t \in \left[t_n^e, t_{n+1}^m\right) \cap [T, \infty), \forall n$. Likewise, for the case when $\sigma_m = 1$, (47) can be bounded above by utilizing Assumption 1, Property 2, and Young's Inequality as

$$\begin{aligned} \dot{V} \overset{\text{a.e.}}{\leq} & -\left(\alpha - \tfrac{1}{2}\right) e_1^2 - \left(c_b k_2 - \tfrac{1}{2}\right) e_2^2 \\ & -k_3 \lambda_e \tilde{\theta}_e^T \tilde{\theta}_e - k_4 \lambda_m c_b \tilde{\theta}_m^T \tilde{\theta}_m, \end{aligned} \tag{53}$$

$\forall t \in [t_n^m, t_n^e) \cap [T, \infty), \forall n$. An overall upper bound for both (52) and (53) can be obtained by using (41) as

$$\dot{V} \overset{\text{a.e.}}{\leq} -\frac{\delta}{\lambda_2} V, \tag{54}$$

$\forall t \in [T, \infty)$. From (52) and (53), (40) is a common Lyapunov function for the case when $\sigma_e = 1$ and the case when $\sigma_m = 1$. Solving the differential inequality in (54) and using (41) yields

$$\|z(t)\| \leq \sqrt{\frac{\lambda_2}{\lambda_1}} \|z(T)\| \exp\left(-\frac{\delta}{2\lambda_2}(t - T)\right), \forall t \in [T, \infty). \tag{55}$$

Combining the result in (55) with (50) from Theorem 1 yields the exponential bound for all $t \in [0, \infty)$ shown in (51). Using (42) and (55) it can be shown that $e_1, e_2, \tilde{\theta}_e, \tilde{\theta}_m \in \mathcal{L}_\infty$. Following a similar development as in Theorem 1 it can be shown that $u_{mot}, u_{FES} \in \mathcal{L}_\infty$ and the remaining signals are bounded. ■

V. Simulation

To demonstrate the performance of the controllers in (37) and (38) and the update laws in (17) and (18) a preliminary numerical simulation was performed using the dynamics in (8). The desired trajectory was designed as

$$q_d(t) = \frac{\pi}{9} + \frac{7\pi}{36}\left[1 - \cos\left(\frac{\pi}{10} t\right)\right],$$

and the initial forearm position and velocity were selected as $q(0) = \frac{\pi}{9}$ rad and $\dot{q}(0) = 0$ rad/s. The initial parameter estimates were selected as $\hat{\theta}_e = \hat{\theta}_m = [0, 0, 0, 0, 2]^T$. The following control gains were used $k_1 = 15$, $k_2 = 25$, $k_3 = 5$, $k_4 = 10$, $k_m = 20$, $\lambda = 0.01$, $\alpha = 1$, $\triangle t = 0.5$s, $N_m = N_e = 500$, $\Gamma_m = diag\{95, 20, 0.05, 0.05, 15\}$, $\Gamma_e = diag\{210, 5, 0.05, 0.01, 2\}$.

The following plots show the results of the simulation. The position and velocity tracking errors are shown in Figure 1.

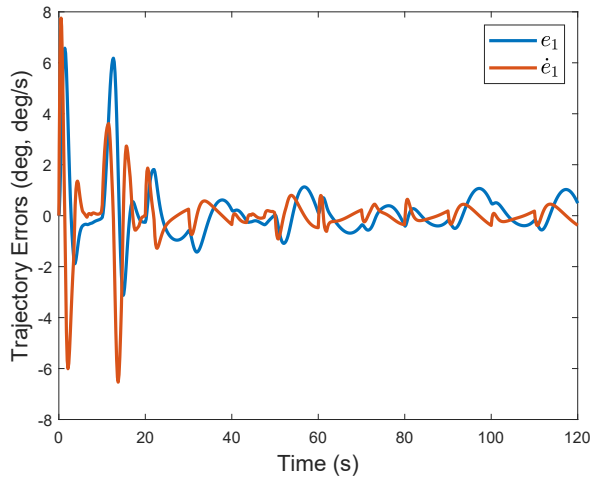

Fig. 1. Tracking errors.

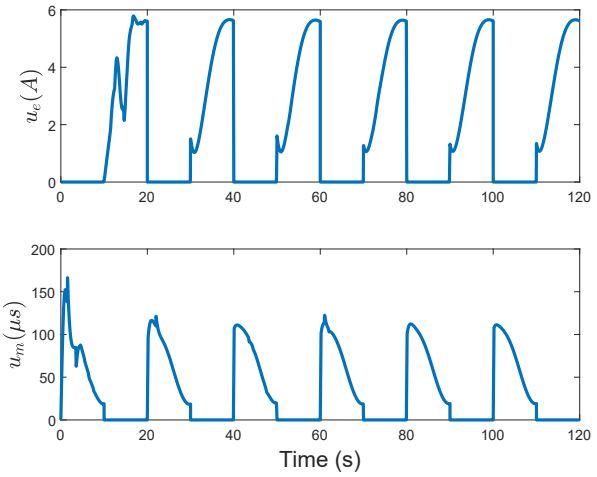

Fig. 2. Control inputs.

The control inputs, u_m and u_e, are shown in Figure 2. The adaptive parameter estimates versus the actual parameters for both the motor and FES subsystems are shown in Figure 3. The parameter estimate errors for both subsystems are shown in Figure 4. The minimum eigenvalue plot for both subsystems is shown in Figure 5.

The position and velocity errors over the entire simulation were 0.14 ± 1.17 deg and 0.004 ± 1.18 deg/s. The root mean square (RMS) position error and velocity errors were 1.18 deg and 1.18 deg/s, respectively over the simulation. The simulation demonstrates the ability of the designed control system to yield small tracking errors and to estimate the parameters of each subsystem. The parameter estimates could be improved by increasing the duration of the simulation or by using more advanced methods to increased the minimum eigenvalue of each subsystem, such as is discussed in [19], [23], and [24]. Additionally, the trajectory could be modified to further excite the system.

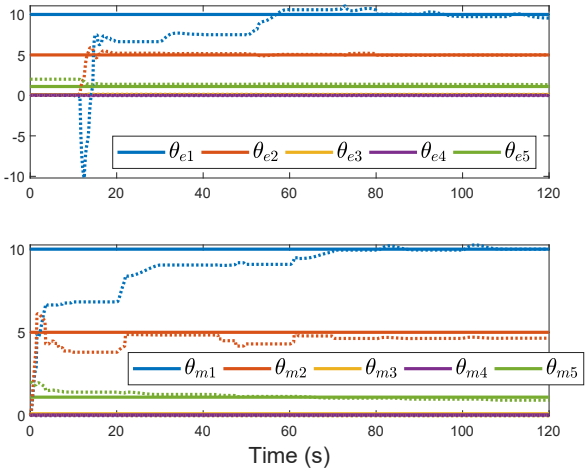

Fig. 3. Parameter estimates for both subsystems. The solid lines indicate the actual parameter values and the dotted lines indicate the parameter estimate.

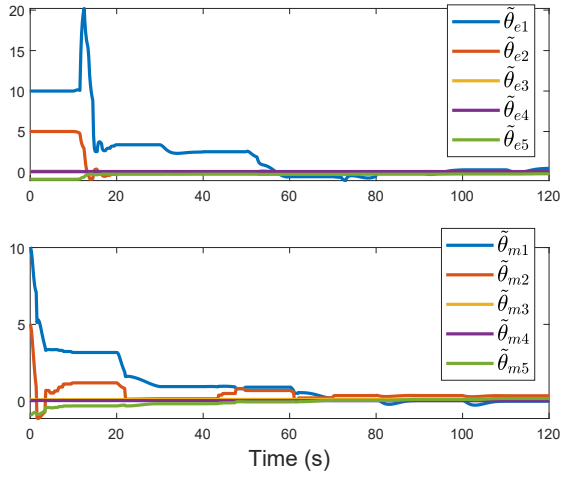

Fig. 4. Parameter estimate errors for both subsystems.

VI. Conclusion

A data-based ICL controller was developed for a switched, motorized FES-induced biceps curl exercise. A Lyapunov-based stability analysis guaranteed both exponential trajectory tracking and opportunistic parameter identification. The developed ICL formulation allows for a more mild FE condition for learning instead of the PE condition and for the dynamics of both the machine and the person to be identified without the need to know the angular acceleration of the elbow joint. Adaptive FES controllers can potentially lower the high-gain/high-frequency inputs from traditional robust controllers and replace them with feedforward adaptive components, which can help to delay the onset of fatigue. A preliminary simulation is perfomed to validate the performance of the designed control system and yields an average position error of 0.14 ± 1.17 deg and an average velocity error of 0.004 ± 1.18 deg/s. Future work will allow for switching between multiple

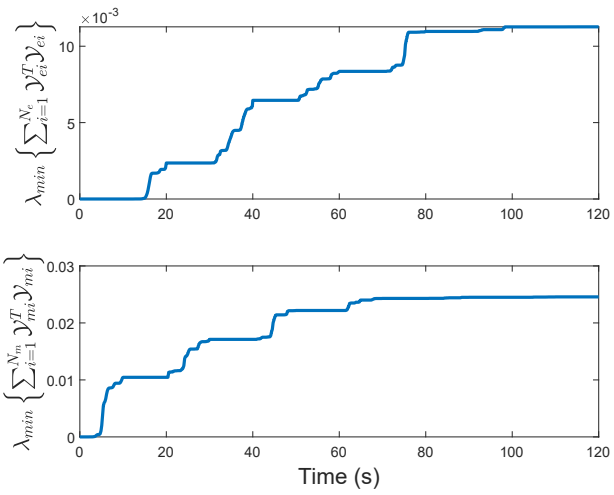

Fig. 5. Parameter estimates errors for the concurrent learning controller (Controller 2).

electrodes by spatially switching stimulation as the muscle geometry changes with joint angle to improve efficiency and further reduce fatigue [5].

REFERENCES

[1] M. J. Bellman, R. J. Downey, A. Parikh, and W. E. Dixon, "Automatic control of cycling induced by functional electrical stimulation with electric motor assistance," *IEEE Trans. Autom. Science Eng.*, vol. 14, no. 2, pp. 1225–1234, April 2017.

[2] C. Rouse, C. Cousin, V. H. Duenas, and W. E. Dixon, "Varying motor assistance during biceps curls induced via functional electrical stimulation," in *Proc. ASME Dyn. Syst. Control Conf.*, 2018.

[3] E. J. Gonzalez, R. J. Downey, C. A. Rouse, and W. E. Dixon, "Influence of elbow flexion and stimulation site on neuromuscular electrical stimulation of the biceps brachii," *IEEE Trans. Neural Syst. Rehabil. Eng.*, vol. 26, no. 4, pp. 904–910, April 2018.

[4] C. Rouse, C. Cousin, V. H. Duenas, and W. E. Dixon, "Switched motorized assistance during switched functional electrical stimulation of the biceps brachii to compensate for fatigue," in *IEEE Conf. Dec. Control*, 2017, pp. 5912–5918.

[5] C. Rouse, V. H. Duenas, C.Cousin, A. Parikh, and W. E. Dixon, "A switched systems approach based on changing muscle geometry of the biceps brachii during functional electrical stimulation," *IEEE Control Syst. Lett.*, vol. 2, no. 1, pp. 73–78, 2018.

[6] Z. Li, M. Hayashibe, C. Fattal, and D. Guiraud, "Muscle fatigue tracking with evoked emg via recurrent neural network: Toward personalized neuroprosthetics," *Comput. Intell.*, vol. 9, no. 2, pp. 38–46, 2014.

[7] E. S. Idsø, T. Johansen, and K. J. Hunt, "Finding the metabolically optimal stimulation pattern for FES-cycling," in *Proc. Conf. of the Int. Funct. Electrical Stimulation Soc.*, Bournemouth, UK, Sep. 2004.

[8] N. A. Alibeji, N. A. Kirsch, and N. Sharma, "A muscle synergy-inspire adaptive control scheme for a hybrid walking neuroprosthesis," *Front. Bioeng. Biotechnol.*, vol. 3, no. 203, pp. 1–13, Dec. 2015.

[9] R. J. Downey, T.-H. Cheng, M. J. Bellman, and W. E. Dixon, "Switched tracking control of the lower limb during asynchronous neuromuscular electrical stimulation: Theory and experiments," *IEEE Trans. Cybern.*, vol. 47, no. 5, pp. 1251–1262, May 2017.

[10] I. Karafyllis, M. Malisoff, M. de Queiroz, M. Krstic, and R. Yang, "Predictor-based tracking for neuromuscular electrical stimulation," *Int. J. Robust Nonlin.*, vol. 25, no. 14, pp. 2391–2419, 2015.

[11] M. Ferrarin, F. Palazzo, R. Riener, and J. Quintern, "Model-based control of FES-induced single joint movements," *IEEE Trans. Neural Syst. Rehabil. Eng.*, vol. 9, no. 3, pp. 245–257, Sep. 2001.

[12] N. Sharma, C. M. Gregory, M. Johnson, and W. E. Dixon, "Closed-loop neural network-based nmes control for human limb tracking," *IEEE Trans. Control Syst. Tech.*, vol. 20, no. 3, pp. 712–725, 2012.

[13] Z. Hussain, M. A. Zaidan, M. O. Tokhi, and R. Jailani, "The adaptive control of fes-assisted indoor rowing exercise," *Proc. Int. Automatic Control Conference (CACS)*, 2009.

[14] V. Duenas, C. A. Cousin, V. Ghanbari, E. J. Fox, and W. E. Dixon, "Torque and cadence tracking in functional electrical stimulation induced cycling using passivity-based spatial repetitive learning control," *Automatica*, to appear.

[15] V. H. Duenas, C. A. Cousin, A. Parikh, P. Freeborn, E. J. Fox, and W. E. Dixon, "Motorized and functional electrical stimulation induced cycling via switched repetitive learning control," *IEEE Trans. Control Syst. Tech.*, vol. 27, no. 4, pp. 1468–1479, 2019.

[16] V. H. Duenas, C. A. Cousin, C. Rouse, E. J. Fox, and W. E. Dixon, "Distributed repetitive learning control for cooperative cadence tracking in functional electrical stimulation cycling," *IEEE Trans. Cybern.*, vol. 50, no. 3, pp. 1084–1095, 2020.

[17] K.-M. Wang, T. Schauer, H. Nahrstaedt, and J. Raisch, "Iterative learning control of cadence for functional electrical stimulation induced cycling in paraplegia," in *Proc. Conf. of the Int. Funct. Electrical Stimulation Soc.*, Sep. 2009, pp. 71–73.

[18] C. Cousin, P. Deptula, C. Rouse, and W. E. Dixon, "Cycling with functional electrical stimulation and adaptive neural network admittance control," in *Proc. Am. Control Conf.*, 2019, pp. 1742–1747.

[19] Z. Bell, J. Nezvadovitz, A. Parikh, E. Schwartz, and W. Dixon, "Global exponential tracking control for an autonomous surface vessel: An integral concurrent learning approach," *IEEE J. Ocean Eng.*, to appear.

[20] B. D. Anderson, "Adaptive systems, lack of persistency of excitation and bursting phenomena," *Automatica*, vol. 21, no. 3, pp. 247–258, 1985.

[21] S. B. Roy, S. Bhasin, and I. N. Kar, "A uges switched mrac architecture using initial excitation," in *IFAC-PapersOnLine*, vol. 50, no. 1, Jul. 2017, pp. 7044–7051.

[22] G. V. Chowdhary and E. N. Johnson, "Theory and flight-test validation of a concurrent-learning adaptive controller," *J. Guid. Control Dynam.*, vol. 34, no. 2, pp. 592–607, Mar. 2011.

[23] A. Parikh, R. Kamalapurkar, and W. E. Dixon, "Integral concurrent learning: Adaptive control with parameter convergence using finite excitation," *Int J Adapt Control Signal Process*, vol. 33, no. 12, pp. 1775–1787, Dec. 2019.

[24] R. Licitra, Z. I. Bell, E. Doucette, and W. E. Dixon, "Single agent indirect herding of multiple targets: A switched adaptive control approach," *IEEE Control Syst. Lett.*, vol. 2, no. 1, pp. 127–132, January 2018.

[25] N. Fischer, R. Kamalapurkar, and W. E. Dixon, "LaSalle-Yoshizawa corollaries for nonsmooth systems," *IEEE Trans. Autom. Control*, vol. 58, no. 9, pp. 2333–2338, Sep. 2013.

[26] A. F. Filippov, "Differential equations with discontinuous right-hand side," in *Fifteen papers on differential equations*, ser. American Mathematical Society Translations - Series 2. American Mathematical Society, 1964, vol. 42, pp. 199–231.